



Journal of Advanced Research in Applied Mechanics

Journal homepage:
https://semarakilmu.com.my/journals/index.php/appl_mech/index
ISSN: 2289-7895



Finite Element Analysis for Aluminium Alloy 7075-T6 Subjected to the Bending-Torsional Variable Phase of Fatigue Loading

Batool Mardan Faisal¹, Emad Jebur Yousif², Emad Kamil Hussein², Hussein Kadhim Sharaf^{3,4,*}, Thiago Santos⁵, Carolyn Santos⁵, Kaltoum Belhassan⁶

¹ Mechanical Engineering Department, College of Engineering, Wasit University, Wasit, Iraq

² Mechanical Power Engineering Department, Mussaib Technical College, Al Furat Al Awsat Technical University, 51006, Babil, Iraq

³ Aeronautical Department, Bilad Alrafidain University College, Baquba, Iraq

⁴ Dijlah University College, Iraq

⁵ Technology center, Federal University of Rio Grande do Norte, Av. Prof. Sen. Salgado Filho, 3000, Natal, Rio Grande do Norte, 59072-970, Brazil

⁶ Independent researcher, Dewsbury, WF13 4QP, West Yorkshire, United Kingdom

ARTICLE INFO

Article history:

Received 7 October 2024

Received in revised form 7 November 2024

Accepted 14 November 2024

Available online 30 November 2024

Keywords:

Fatigue behaviour; mixing phase load; Al alloy; FEM; life prediction

ABSTRACT

In this study, the fatigue behaviour of the alloy structure of Aluminium alloy 7075-T6 is investigated numerically. Three main factors were taken into account when researching the alloy composition of aluminium alloy 7075-T6: life prediction, damage indicator, and Biaxiliray indexation. A prediction of life expectancy seems to be the most reliable indication. Experiments have been carried out with the stress totally inverted as the variable in order to determine whether or not the phenomena of exhaustion can be described by the theory proposed by Goodman. It was determined that the dynamic load of 100 kilonewtons (kN) and 1100 nanometers (Nm) was used in order to produce estimates for these characteristics. In order to assist us in gaining a better understanding of these characteristics, it has approximated them by making use of the dynamic load that was applied. An increase in the main force to 100 kilonewtons would bring the expected lifetime up to 141 cycles, according to the findings of the computer research. In this regard, the findings of the inquiry provided evidence. The findings demonstrated that this is really the case. The Biaxiliray indexation obtained a value of 0.46 when subjected to the same stress conditions. The numerical results demonstrated that the damage is obvious during the first 10E32 cycles of stress, which is in addition to the research that have been conducted on damage indicators. These findings were demonstrated not just through theoretical study of the damage indicator but also via practical numerical data.

1. Introduction

In consideration of two factors—namely, the growing demand for precise residual fatigue life estimations of aeronautical structures and the implementation of damage tolerance design concepts—research on fatigue damage onset and propagation under realistic multiaxial fatigue loading scenarios is becoming an increasingly relevant area of study. It is possible for multiaxiality to

* Corresponding author.

E-mail address: hk.sharaf92@gmail.com

<https://doi.org/10.37934/aram.128.1.6271>

be caused by a wide variety of factors, such as complicated geometry, residual stresses, fracture direction, external multiaxial loads, and many others [1,2].

When it comes to the phenomenon of fracture formation under pure mode I and mode II stress, there have been a multitude of scientific investigations that have been conducted [3,4]. Mixed-mode multiaxial fatigue loadings, on the other hand, are the root cause of many component failures. External loading may be seen in engineering in the form of fractures that originate in the transverse plane from the surface of a tube shaft and are produced by the combination of bending force and torsional force [5].

Rotorcraft and fixed-wing aircraft components are also vulnerable to bending-torsional fatigue, which can manifest over a wide range of stress amplitude ratios. Biaxial strains caused by internal pressure can also damage pipes, tubes, and pressure vessels. Shear pressures from torque and axial stresses from bending are the two forms of stresses that may be applied to a vehicle's gearbox shaft [6,7]. Cracks caused by natural weariness tend to emerge in a mixed-mode fashion in the actual world [8]. This is because, in less-than-ideal environments, structures and components are often subjected to complicated multiaxial loads. Anticipating the fracture course or measuring crack growth at different phases of propagation becomes problematic under mixed-mode settings due to the non-self-similar propagation of a fatigue crack. The reason behind this is that the crack does not move in a straight line [8]. Estimating the material's fatigue life and/or tracking the growth of fractures becomes a laborious and time-consuming task under these conditions. Researching the features of fatigue damage under such complicated loading situations is crucial for making correct forecasts about their service life, damage initiation, and fracture development behavior [9].

As a loading condition, uniaxial pressures have been used in the vast majority of research that have investigated fatigue damage initiation and development [10]. Due to the scarcity of research on multiaxial loading, most of what little is known has focused on axial-torsion coupling. Experiments on this connection have used either static loadings or cyclic loadings in combination with each other [11]. Researchers have not looked at how metals react to fatigue when bending and torsional loads are applied at the same time very much [12]. To investigate the combined effects of bending and torsional force, it is likely that [13] was the first to employ a solid steel cylindrical bar. I think this has to be looked at more. An intricate fixture design was employed to impart stresses, and a single loading arm was used to transfer the total load to the specimen [14]. To do this, we adjusted the arm's angle of rotation with respect to the specimen in question. To do this, the loading arm's angle of orientation might be adjusted. It was for this reason that we were able to separate the applied force into its bending and twisting components. Using the orientation mismatch as an advantage allowed this to happen [15].

Multiple authors in the same body of work repeated the first experiment in a setting that was quite similar to the one used for the following experiments [16,17]. Scientists investigated four distinct permutations of the 76S-T61 aluminum alloy. AA 6068 and AA 2017A were the subjects of research in [18-20], respectively, while 18G2A and 10HNAP were the steel grades utilized. Grades of steel were utilized by both authors [21,22]. All of these research [23,24] found that the fatigue life or endurance limit of cylindrical solid specimens could be determined using the stress-life method. Still, not a single one of the published findings clarified how the examined materials' cracks propagated or how damage started. Fatigue crack analysis involving mixed mode loading requires both of these features to be present [25].

Whenever materials are subjected to a combination of bending and torsion stress, there is a dearth of experimental data about the manner in which damage is begun or the manner in which cracks spread [26]. According to the findings of [27], who investigated the fatigue behavior of solid cylindrical Al 6082-T6 under entirely reversed bending-torsion circumstances, fracture initiation takes

place in mode II in a location of highest bending stress. This is despite the fact that the crack propagates under mode I pressures the majority of the time. They arrived to this interpretation as a result of their examination of the fatigue behavior of the material. When the torque that is applied is more than one, the surface of the gauge develops an excessive number of fractures that are aligned with the direction in which the extrusion is occurring. It did not make a difference to these results whether the loading was in phase or out of phase; the effects were the same in both instances. As stated by the author [28], who investigated the behavior of minute A533B steel fractures under inphase and 90° out-of-phase stress, the rate of fracture propagation altered in a linear fashion with the crack size. The results of his research were published in the journal *Materials Science and Engineering* [29].

However, the orientations in which the fractures developed were different depending on whether the stress was in-phase or 90 degrees out-of-phase. They spread in different directions. In the plane that was subjected to the maximum shear strain, each and every one of the fractures started to appear. When the strain level or the ratio of shear to bending strain decreased, the fracture moved from the plane of highest shear strain to the plane of maximum normal strain with in-phase loading. This occurred when the fracture was subjected to in-phase loading. On the other hand, the fracture continued to spread along the plane in which it had been initially positioned even when the loading was in phase with each other. Because of an in-phase loading, the fracture moved from the shear strain plane to the normal strain plane from its previous location. Along these same lines, a number of studies [30] have utilized specimens that had notches attached to them.

According to the authors of [31], fractures occurred and advanced along the lines of highest shear stress and main stress amplitudes. This was the case. It was via the use of solid round steel bars that had a semicircular groove around their perimeter that the finding was discovered. For the purpose of carrying out these observations, the round and substantial steel bars were utilized [32]. In the 90-degree out-of-phase testing with 0.5, fracture propagation was seen on planes that were oriented between the planes that had the greatest shear stress amplitude and the planes that had the largest main stress amplitude [33]. This was done with the intention of determining the direction in which the fracture was expanding. Research conducted on the fatigue behavior of high-strength steel lateral notched round bars revealed that the fracture surfaces of the bars had developed a number of cracks [34].

As the normal stress amplitude was raised, the crack initiation time and crack development rate were also enhanced. For both fissures, this was true. An important knowledge vacuum regarding the micromechanisms underlying fatigue fracture remains because the aforementioned studies failed to adequately investigate the characteristics of crack initiation and propagation behavior under coupled bending-torsional stress. In addition, specific, complicated test sets were used for all bending-torsion loading experiments up to this time. The outcome was a less trustworthy load application method and the inability to achieve uniformity in the testing procedure [35].

As a result, in order to accomplish the objectives of this study, a finite element analysis was carried out on the aluminum alloy 7075-T6 while it was being subjected to the bending-torsional variable phase of fatigue loading.

2. Methodology

2.1 Mechanical Properties

In order to meet the requirements of this investigation into bending and torsional fatigue, the material was acquired in the form of cylindrical bars that were fabricated from the aluminum alloy 7075-T6 (Table 1). In the manufacturing of aircraft structural components, in the car sector, and in a

variety of other high-strength applications, this alloy is commonly utilized. In order to conduct this investigation, the material was obtained. According to the material's specifications, the ultimate tensile strength of the material is reported to be 572 MPa, while the modulus of elasticity of the material is described as 71.7 GPa. In accordance with the specifications, the material has a yield strength of 503 MPa. It was agreed upon by the manufacturer that these data would be provided for the product. In line with the ASTM standard for B211, this material has a Brinell hardness value of 150, and its chemical compositions are in compliance with the standard.

Table 1

Mechanical properties of alloy structure of the aluminum alloy 7075-T6			
Modulus of elasticity (GPa)	Ultimate tensile stress (MPa)	Poisson ratio	Density (g/cm ³)
71.7	572	0.32	1.95

2.2 Meshing and Geometry of Aluminum Alloy 7075-T6

With the assistance of mesh, the meshing technique that was applied to the current circumstance was carried out. Once an aluminum alloy 7075-T6 has been produced from an unlimited number of particles, it must next go through the meshing process in order to be considered complete. This action is taken in order to bring the total number of particles down to a level that is more controllable inside the system. For the purpose of obtaining findings that could be depended upon, a very small mesh was constructed by making use of a grid structure that had been established. The manufacturing of the mesh was made possible as a result of this issue. By combining a combination of curvature size with a coarse mesh and element size with face meshing, we were able to achieve the desired outcome of a tiny mesh. This was accomplished with the aid of sizing management. With the help of this integrated strategy, we were able to arrive at the intended conclusion. As a direct result of this, it was feasible to produce the tiny mesh that was necessary. The creation of binary nodes for the wedge in each and every one of its zones has resulted in the computation of a grand total of 46577 binary nodes. This is the result of the construction of binary nodes.

Figure 1 is an illustration of the type of mesh that may be found in a place that only has two dimensions. The symmetry of the aluminum alloy 7075-T6 that has been produced up to this point is the single trait that distinguishes the aluminum alloy 7075-T6 that has been generated up to this point. Because of the symmetric nature of the three-dimensional wedge, this is the case. The reason behind this is that the symmetry of the three-dimensional wedge was discovered by coincidence, which is the rationale behind this scenario. There are three distinct types of boundary conditions that were applied by the authors of this study during the whole of their inquiry.

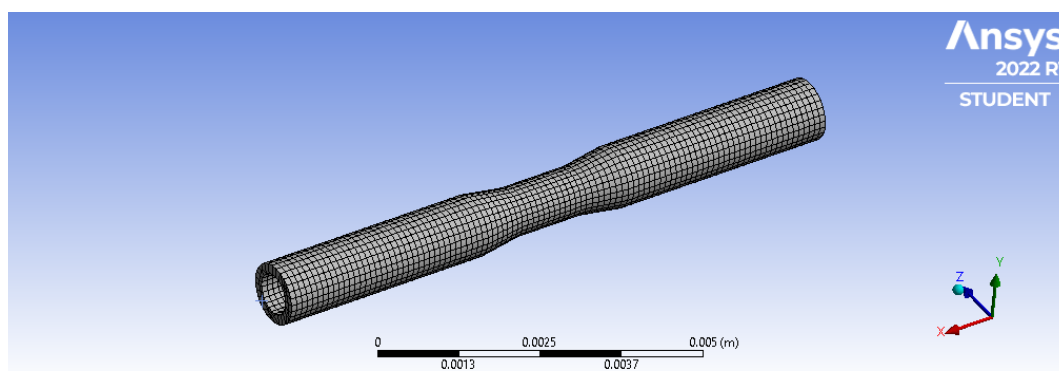


Fig. 1. Meshed alloy of AA2024-T of the AA2024-T4

2.3 Boundary Conditions

This examination included a monotonic fatigue test, which was carried out at several points along the process. In order to achieve the desired level of pressure, a combination of 110 kilonewtons (kN) and 1100 newton metres (newton metres) was employed. For the objective of this inquiry, fatigue tests were carried out by utilizing a method that was created from a prosthetic model that was used in the actual world. Specimens were loaded concurrently while bending-torsion stress was being applied to them throughout the experiment [14]. An aluminum alloy 7075-T6 was used in the construction of a sample that was subjected to fatigue testing over the course of this investigation.

2.4 Convergence Analysis

The strategy that has been selected to be employed in the empirical investigation that has been carried out regarding the link is referred to as a convergence test on the part of the researchers. The decision to go with this approach was made since, it was regarded to be the most suitable option. The research that was indicated before has now been completed as shown in Figure 2. This decision was made. Following significant deliberation and reaching an agreement, this conclusion was brought about. It was determined that this plan would be implemented. It was via the employment of the consensus technique that this outcome was finally achieved. All of the steps involved in achieving convergence have been completed, and the process is now considered to be concluded. The achievement of this goal was achieved by taking into consideration two different possibilities. As a consequence of this, it may be concluded that convergence has been achieved. When we started the process of counting cycles for the first answer, we found that there were 1.4 millimeters worth of them there. This was the first thing that we noticed.

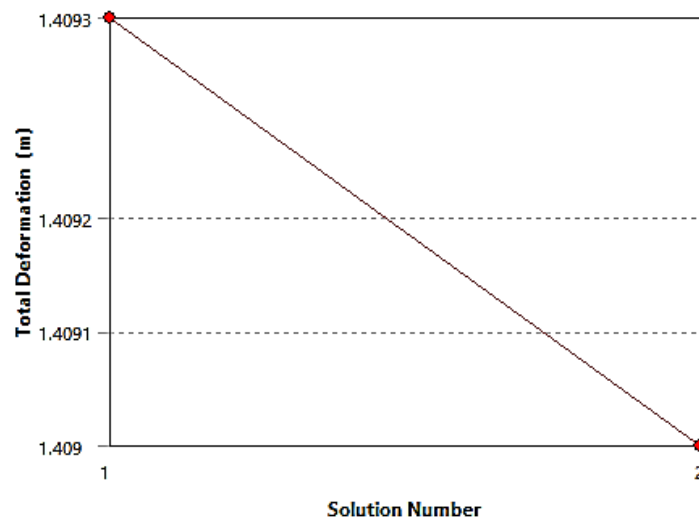


Fig. 2. Convergence analysis of the alloy of Al-7075

3. Results

3.1 Life Predictions

We expected that fatigue spacemen constructed from Al-7075 Alloy would continue to execute their tasks for a specific length of time after being subjected to a changing stress. This hypothesis was developed for the aim of this inquiry. Research was conducted to evaluate the prediction of longevity. This study was carried out as a consequence of the application of a torsional stress in addition to a

fatigue load of 110 KN. The findings of this inquiry are provided in Figure 3, as can be seen in the figure of results.

Throughout the length of the simulation session, the Static structural tool in the ANSYS program was consistently engaged. This tool may be accessed inside the application. According to the findings of computational studies, the specimen of the Al-7075 alloy structure that has been reinforced with kenaf particles has demonstrated the capacity to withstand stresses of up to about one e6 cycles. In light of this fact, it is strongly suggested that the existing analysis be rendered incorrect at some point during the 141st cycle.

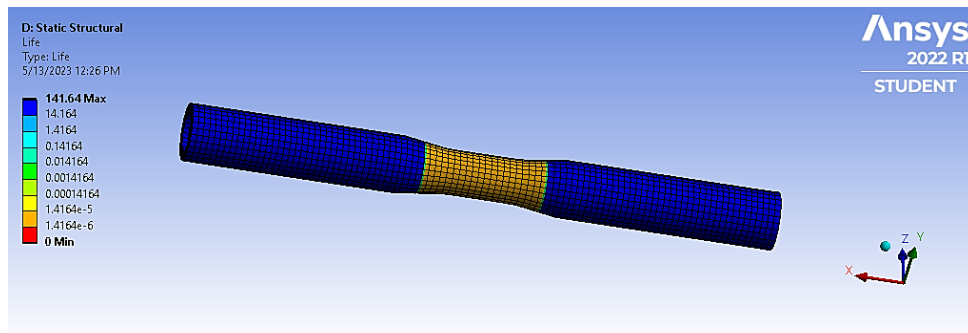


Fig. 3. Life prediction of the current geometry

3.2 Biaxiality Indexation

The biaxiality suggestion in the current investigation sheds light on both the stress condition that was experienced over the Al-7075 alloy as well as the manner in which the data ought to be interpreted. This information is also included in the biaxiality indicator, in addition to the findings that were obtained.

In this particular instance, the biaxiality indicator is discovered by disregarding the main stress that is the closest to zero in magnitude and dividing the principal stress that has a greater magnitude by the principal stress that has a smaller size. To put it another way, the computation does not take into account the primary stress of the smallest size. By doing this particular calculation, it is possible to determine whether or not the material is biaxial. In the same way that uniaxial stress operates in just one direction, unidirectional stress, which is also frequently referred to as uniaxial stress, follows the same pattern. The biaxiality indicator reached a value of 1 when the alternative load of 110 KN was applied to the system. There has been a change in the value of the biaxiality indicator, which is now 0.4308. As can be seen in Figure 4, the results of the simulation demonstrated that the biaxiality signal at the tips was the most significant that was occurring. All of this was demonstrated to us by the simulation.

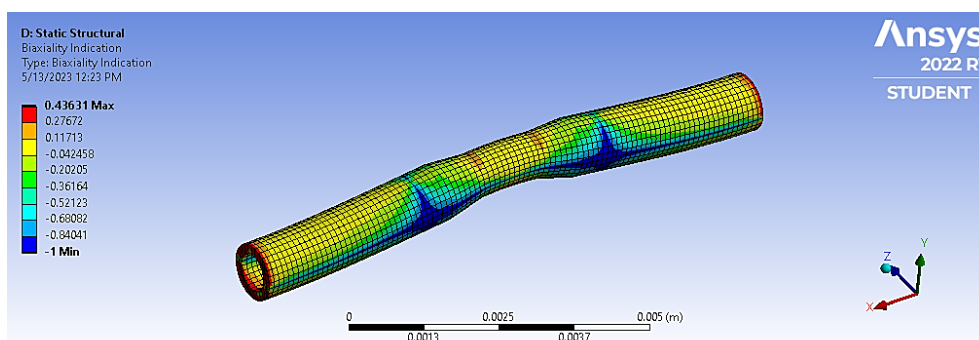


Fig. 4. Biaxiality indexation due to the applied load

3.3 Damage Predictions

Figure 5, which depicts the possibility that the structure may experience damage as a result of loading, is an illustration of this concept. As a result of this, it has been demonstrated that the likelihood that this is a reality is true. It has been determined that specimens have been loaded with a force that is comparable to 110 key moments (KN) in order to complete the computational examination of the Al-7075 alloy that was utilized in the 3D fatigue spacemen. Therefore, it is up to them to share the responsibility of bearing the weight of this commitment. $10E32$ is the lowest number of cycles that must be completed before the maximum damage potential is attained, and the maximum number of cycles that must be completed in order to obtain the maximum damage potential is also $10E32$. However, the minimum number of cycles that must be completed is $10E32$. Both of these figures are in conformity with the highest harm potential that may be occurring.

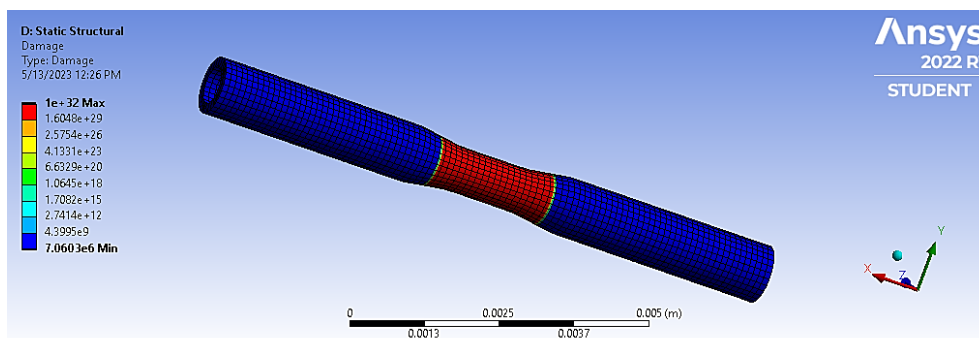


Fig. 5. Damage explanation due to the applied load

3.4 Equivalent Alternative Stress

The portions of the alloy specimens that were subjected to stress as a result of the simulated 110 KN force have been identified. Through the identification of the particular places in concern, the outcomes of the simulation have made this a feasible possibility. Over the entirety of the material being evaluated, the strain is applied in a consistent manner along a single axis. Consequently, this ensures that the pressure is administered in a consistent manner. The fillet of the alloy fatigue sample was subjected to alternating stresses that were focused at its body. There, these pressures were particularly noticeable and pronounced. Following the completion of the study, it was determined that the fillet sections of the specimen were subjected to a maximum alternative stress of 318.78 MPa. This pricing was determined as a result of the investigation that was conducted. The alternate stress that is considered to be the lowest acceptable level is 318 MPa, as shown in Figure 6.

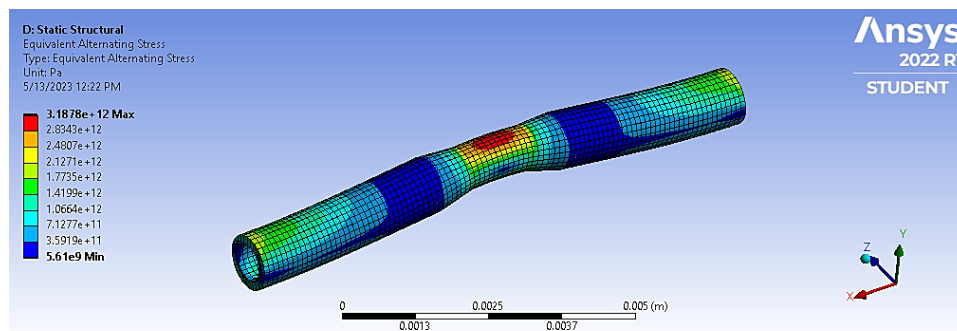


Fig. 6. Numerical results of Equivalent alternative stress

4. Conclusions

An investigation of the fatigue behavior of the alloy structure of the aluminum alloy 7075-T6 is carried out with the assistance of numerical analysis. During the course of the research that was carried out on the composition of the aluminum alloy 7075-T6, the three most important factors that were taken into consideration were life prediction, damage indicator, and Biaxial indexation. The prediction of the life expectancy was the only other metric that was more accurate than the one that was used originally. For the purpose of determining whether or not the phenomenon of weariness can be represented by the idea that was provided by Goodman, experiments have been carried out in which the stress has been fully reversed as the variable. The application of a dynamic load with a magnitude of 100 kilonewtons (kN) and 1100 nanometers (Nm) led to the creation of estimations for these parameters. This was accomplished by applying the load. They were estimated by making use of the dynamic load that was applied in order to get a more in-depth understanding of the characteristics that they possessed.

After doing the study on the computer, it was found that increasing the primary force to 100 KN would lead to an increase in the predicted lifetime to 141 cycles. This was calculated based on the findings of the research. This claim was provided with evidentiary backing by the findings of the investigation that ended up being conducted. Taking into consideration all of these facts, this assertion was comprehensively supported. The value of the biaxial indexation reached 0.46 when it was subjected to the identical stress conditions as it had been before. Additionally, the research that explored damage indicators indicated that the damage is obvious during the first 1032 cycles that the material is subjected to while it is under stress. This was proved by the numerical data. This was not only established via the theoretical analysis of the damage indicator, but it was also demonstrated through the statistical data that was really collected.

References

- [1] Luo, Zhengbo, Huaihai Chen, and Xudong He. "Influences of correlations between biaxial random vibrations on the fatigue lives of notched metallic specimens." *International Journal of Fatigue* 139 (2020): 105730. <https://doi.org/10.1016/j.ijfatigue.2020.105730>
- [2] Karimian, Seyed Fouad, Hugh A. Bruck, and Mohammad Modarres. "Thermodynamic entropy to detect fatigue crack initiation using digital image correlation, and effect of overload spectrums." *International Journal of Fatigue* 129 (2019): 105256. <https://doi.org/10.1016/j.ijfatigue.2019.105256>
- [3] Singh, Abhay K. "Micro-and macro-scale characterization of fatigue damage behavior in metallic materials under constant and variable amplitude multiaxial loading." PhD diss., Arizona State University, 2021.
- [4] Singh, Abhay K., Siddhant Datta, Aditi Chattopadhyay, Jaret C. Riddick, and Asha J. Hall. "Fatigue crack initiation and propagation behavior in Al-7075 alloy under in-phase bending-torsion loading." *International Journal of Fatigue* 126 (2019): 346-356. <https://doi.org/10.1016/j.ijfatigue.2019.05.024>
- [5] Singh, Abhay K., Siddhant Datta, Aditi Chattopadhyay, Asha Hall, and Jaret C. Riddick. "Fatigue damage initiation and propagation in Al-7075 under combined bending and torsion loading." In *AIAA Scitech 2019 Forum*, p. 0412. 2019. <https://doi.org/10.2514/6.2019-0412>
- [6] Sharaf, Hussein Kadhim, M. R. Ishak, S. M. Sapuan, and N. Yidris. "Conceptual design of the cross-arm for the application in the transmission towers by using TRIZ-morphological chart-ANP methods." *Journal of Materials Research and Technology* 9, no. 4 (2020): 9182-9188. <https://doi.org/10.1016/j.jmrt.2020.05.129>
- [7] Xu, Z. K., Baolin Wang, P. Zhang, X. Z. Gu, and Z. F. Zhang. "Crack branching and deflection in AISI 4340 steel under cyclic torsional loading." *Materials Science and Engineering: A* 863 (2023): 144561. <https://doi.org/10.1016/j.msea.2022.144561>
- [8] Ouyang, Yuanwen, Hongbo Liu, Jiaojie Ying, Jianxiong Zhao, Xiaowei Liu, and Zhenfei Liu. "Study on the behavior of assembled T-shaped aluminum alloy specimens under axial compression." *Metals* 13, no. 5 (2023): 919. <https://doi.org/10.3390/met13050919>

- [9] Sharaf, Hussein Kadhim, Shahad Alyousif, Najlaa Jasim Khalaf, Ahmed Faeq Hussein, and Mohammed Khudhair Abbas. "Development of bracket for cross arm structure in transmission tower: Experimental and numerical analysis." *New Materials, Compounds and Applications* 6, no. 3 (2022): 257-275.
- [10] Alilakbari, K., Mohammad Imanparast, and R. Masoudi Nejad. "Microstructure and fatigue fracture mechanism for a heavy-duty truck diesel engine crankshaft." *Scientia Iranica* 26, no. 6 (2019): 3313-3324. <https://doi.org/10.24200/sci.2018.50964.1939>
- [11] Majzoobi, G. H., and P. Azhdarzadeh. "Estimation of axial fretting fatigue life at elevated temperatures using critical distance theory." *Surface Review and Letters* 25, no. 03 (2018): 1850067. <https://doi.org/10.1142/S0218625X18500671>
- [12] Luo, Zhengbo, Huaihai Chen, and Xudong He. "Influences of correlations between biaxial random vibrations on the fatigue lives of notched metallic specimens." *International Journal of Fatigue* 139 (2020): 105730. <https://doi.org/10.1016/j.ijfatigue.2020.105730>
- [13] Singh, Abhay K. "Micro-and macro-scale characterization of fatigue damage behavior in metallic materials under constant and variable amplitude multiaxial loading." PhD diss., Arizona State University, 2021.
- [14] Sharaf, Hussein Kadhim, M. R. Ishak, S. M. Sapuan, N. Yidris, and Arash Fattahi. "Experimental and numerical investigation of the mechanical behavior of full-scale wooden cross arm in the transmission towers in terms of load-deflection test." *Journal of Materials Research and Technology* 9, no. 4 (2020): 7937-7946. <https://doi.org/10.1016/j.jmrt.2020.04.069>
- [15] Mohammadi, Milad, Mohammad Reza Khedmati, and Ehsan Bahmyari. "Elastic local buckling strength analysis of stiffened aluminium plates with an emphasis on the initial deflections and welding residual stresses." *Ships and offshore structures* 14, no. 2 (2019): 125-140. <https://doi.org/10.1080/17445302.2018.1482061>
- [16] Liu, P. S., and X. M. Ma. "Mechanical investigation on failure modes of reticular porous metal foams under different loadings in engineering applications." *Multidiscipline Modeling in Materials and Structures* 17, no. 4 (2021): 814-840. <https://doi.org/10.1108/MMMS-11-2020-0279>
- [17] Ulas, Hasan Basri, Murat Tolga Ozkan, and Yusuf Malkoc. "Vibration prediction in drilling processes with HSS and carbide drill bit by means of artificial neural networks." *Neural Computing and Applications* 31 (2019): 5547-5562. <https://doi.org/10.1007/s00521-018-3379-3>
- [18] Karimian, Seyed Fouad. "Thermodynamic and information entropy-based prediction and detection of fatigue failures in metallic and composite materials using acoustic emission and digital image correlation." PhD diss., University of Maryland, College Park, 2021.
- [19] Salman, Sadeq, Hussein Kadhim Sharaf, Ahmed Faeq Hussein, Najlaa Jasim Khalaf, Mohammed Khudhair Abbas, Ashham Mohammed Aned, Alaa Abdulazeez Turki Al-Taie, and Mustafa Musa Jaber. "Optimization of raw material properties of natural starch by food glue based on dry heat method." *Food Science and Technology* 42 (2022): e78121. <https://doi.org/10.1590/fst.78121>
- [20] Rafidah, M., M. R. M. Asyraf, N. M. Nurazzi, Shukur Abu Hassan, R. A. Ilyas, T. Khan, Wan Alif Abdul Saad, A. Rashedi, S. Sharma, and Emad Kamil Hussein. "Unlocking the potential of lignocellulosic biomass in road construction: A brief review of OPF." *Materials Today: Proceedings* (2023). <https://doi.org/10.1016/j.matpr.2023.01.103>
- [21] Hussein, Emad Kamil, Kussay Ahmed Subhi, and Tayser Sumer Gaaz. "Effect of Stick-Slip Phenomena between Human Skin and UHMW Polyethylene." *Pertanika Journal of Science & Technology* 29, no. 3 (2021). <https://doi.org/10.47836/pjst.29.3.06>
- [22] Subhi, Kussay Ahmed, Emad Kamil Hussein, Shaymaa Abdul Khader Al-Jumaili, and Zaid Ali Abbas. "Implementation of the numerical analysis of dynamic loads on the composite structure employing the FE method." *Eastern-European Journal of Enterprise Technologies* 1, no. 7 (2022): 115. <https://doi.org/10.15587/1729-4061.2022.253545>
- [23] Jalil, Nawal Aswan Abdul, Hussein Kadhim Sharaf, and Sadeq Salman. "A simulation on the effect of ultrasonic vibration on ultrasonic assisted soldering of Cu/SAC305/Cu joint." *Journal of Advanced Research in Applied Mechanics* 36, no. 1 (2017): 1-9.
- [24] Sharaf, Hussein Kadhim, Sadeq Salman, Marwah H. Abdulateef, Rustem R. Magizov, Vasilii Ivanovich Troitskii, Zaid Hameed Mahmoud, Rafis H. Mukhutdinov, and Harsha Mohanty. "Role of initial stored energy on hydrogen microalloying of ZrCoAl (Nb) bulk metallic glasses." *Applied Physics A* 127 (2021): 1-7. <https://doi.org/10.1007/s00339-020-04191-0>
- [25] Salman, Sadeq, Hussein Kadhim Sharaf, Ahmed Faeq Hussein, Najlaa Jasim Khalaf, Mohammed Khudhair Abbas, Ashham Mohammed Aned, Alaa Abdulazeez Turki Al-Taie, and Mustafa Musa Jaber. "Optimization of raw material properties of natural starch by food glue based on dry heat method." *Food Science and Technology* 42 (2022): e78121. <https://doi.org/10.1590/fst.78121>
- [26] Alwan, Saleemah Abdullah, Karrar Kareem Jawad, Nagham Hameed Abdulkhudhur Alyaseri, Kussay Ahmed Subhi, Emad Kamil Hussein, Ashham Mohammed Aned, Hussein Kadhim Sharaf, Hakeem Hammood Flayyih, Mazen

- Dawood Salman, Thuraya Saadon Abdulrasool, and Rajaa Ali Abed. "The psychological effects of perfectionism on sport, economic and engineering students." *Revista Iberoamericana De Psicología Del Ejercicio Y El Deporte* 18, no. 3 (2023): 330-333.
- [27] Alyaseri, Nagham Hameed Abdulkhudhur, Mazen Dawood Salman, Rabab Wahhab Maseer, Emad Kamil Hussein, Kussay Ahmed Subhi, Saleemah Abdullah Alwan, Jasim Gshayyish Zwaid, Ashham Mohammed Aned, Karrar Kareem Jawad, Hakeem Hammood Flayyih, Hussein Kadhim Sharaf, Nasseer Kassim Bachache, and Rajaa Ali Abed. "Exploring the Modeling of Socio-Technical Systems in the Fields of Sport, Engineering and Economics." *Revista Iberoamericana De Psicología Del Ejercicio Y El Deporte* 18, no. 3 (2023): 338-341.
- [28] Jawad, Karrar Kareem, Nagham Hameed Abdulkhudhur Alyaseri, Saleemah Abdullah Alwan, Emad Kamil Hussein, Kussay Ahmed Subhi, Hussein Kadhim Sharaf, Ahmed Faeq Hussein, Mazen Dawood Salman, Jasim Gshayyish Zwaid, Rajaa Ali Abed, and Ashham Mohammed Aned. "Contingency in Engineering Problem Solving Understanding its Role and Implications: Focusing on the sports Machine." *Revista Iberoamericana De Psicología Del Ejercicio Y El Deporte* 18, no. 3 (2023): 334-337.
- [29] Almagsoosi, Lara Qasim Khanjar, Murtada Taha Eesa Abadi, Hussein Falah Hasan, and Hussein Kadhim Sharaf. "Effect of the volatility of the crypto currency and its effect on the market returns." *Industrial Engineering & Management Systems* 21, no. 2 (2022): 238-243. <https://doi.org/10.7232/iems.2022.21.2.238>
- [30] Abdullah, Yussra Malallah, Ghadeer Salim Aziz, and Hussein Kadhim Sharaf. "Simulate the rheological behaviour of the solar collector by using computational fluid dynamic approach." *CFD Letters* 15, no. 9 (2023): 175-182. <https://doi.org/10.37934/cfdl.15.9.175182>
- [31] Bachi Al-Fahad, Imad O., Hussein Kadhim Sharaf, Lina Nasseer Bachache, and Nasseer Kassim Bachache. "Identifying the mechanism of the fatigue behavior of the composite shaft subjected to variable load." *Eastern-European Journal of Enterprise Technologies* 123, no. 7 (2023). <https://doi.org/10.15587/1729-4061.2023.283078>
- [32] Bachi Al-Fahad, Imad O., Azzam D. Hassan, Batool Mardan Faisal, and Hussein Kadhim Sharaf. "identification of regularities in the behavior of a glass fiber-reinforced polyester composite of the impact test based on ASTM D256 standard." *Eastern-European Journal of Enterprise Technologies* 124, no. 7 (2023). <https://doi.org/10.15587/1729-4061.2023.286541>
- [33] Al-Abbas, Audai Hussein, Jamal Naser, and Emad Kamil Hussein. "Numerical simulation of brown coal combustion in a 550 MW tangentially-fired furnace under different operating conditions." *Fuel* 107 (2013): 688-698. <https://doi.org/10.1016/j.fuel.2012.11.054>
- [34] Rafidah, M., M. R. M. Asyraf, N. M. Nurazzi, Shukur Abu Hassan, R. A. Ilyas, T. Khan, Wan Alif Abdul Saad, A. Rashedi, S. Sharma, and Emad Kamil Hussein. "Unlocking the potential of lignocellulosic biomass in road construction: A brief review of OPF." *Materials Today: Proceedings* (2023). <https://doi.org/10.1016/j.matpr.2023.01.103>
- [35] Santos, Thiago F., Carolyn M. Santos, Mariana Dias, Lucas Zilio, Katia M. Melo, Maria Eduarda Cavalcante, Luiz Filipe Castro, Emad Kamil Hussein, and Marcos Aquino. "Mechanical behavior of natural/synthetic weft-knitted structures commonly used as reinforcement of hybrid composites via full factorial design: Yarn compositions and float stitches." In *Green Hybrid Composite in Engineering and Non-Engineering Applications*, p. 261-283. Singapore: Springer Nature Singapore, 2023. https://doi.org/10.1007/978-981-99-1583-5_15